Proteome Science

RESEARCH

Open Access

Mechanism of the cardioprotective effect of empagliflozin on diabetic nephropathy mice based on the basis of proteomics

Zongchao Yu[1†], Yongping Lu[2†], Mengxian Zhang[3†], Yanshan Lin[1], Tak-sui Wong[1], Baozhang Guan[1], Yu Meng[1], Bo Hu[1], Fan-na Liu[1], Lianghong Yin[1], Yankun Li[4], Han Zhang[4*], Donge Tang[5*] and Yong Dai[6*]

Abstract

Diabetic nephropathy affects a significant proportion of individuals with diabetes, and its progression often leads to cardiovascular disease and infections before the need for renal replacement therapy arises. Empagliflozin has been shown to have various protective effects in cardiovascular disease studies, such as improving diabetic myocardial structure and function, and reducing myocardial oxidative stress. However, the impact of empagliflozin on cardiac protein expression and signaling pathways has not been comprehensively analyzed. To address this gap, we conducted proteome analysis to identify specific protein markers in cardiac tissue from the diabetes model group, including Myh7, Wdr37, Eif3k, Acot1, Acot2, Cat, and Scp2, in cardiac tissue from the diabetes model group. In our drug model, empagliflozin primarily modulates the fat-related metabolic signaling pathway within the heart. Empagliflozin downregulated the protein expression levels of ACOX1, ACADVL and CPT1A in the model group. Overall, our findings demonstrate that empagliflozin provides cardiac protection by targeting metabolic signaling pathways, particularly those related to fat metabolism. Moreover, the identification of cardiac biomarkers in a mouse model of diabetic nephropathy lays the foundation for further exploration of disease biomarkers in cardiac tissue.

Keywords Diabetic nephropathy, Empagliflozin, Proteome

[†]Zongchao Yu, Yongping Lu and Mengxian Zhang contributed equally to this work.

*Correspondence:
Han Zhang
zhangh355@mail2.sysu.edu.cn
Donge Tang
donge66@126.com
Yong Dai
daiyong22@aliyun.com
[1] Department of Nephrology, the First Affiliated Hospital of Jinan University, Guangzhou, China
[2] Department of Nephrology, Center of Kidney and Urology, Seventh Affiliated Hospital, Sun Yat-sen University, Shenzhen, China
[3] Department of Internal Medicine, Humen Hospital, Dongguan City, Guangdong Province, China
[4] Dongguan Maternal and Child Health Care Hospital, Postdoctoral Innovation Practice Base of Southern Medical University, Dongguan, China
[5] Clinical Medical Research Center, Shenzhen People's Hospital, The Second Clinical Medical College of Jinan University, Shenzhen 518020, China
[6] The First Affiliated Hospital, School of Medicine, Anhui University of Science and Technology, Huainan, Anhui, China

Background

The number of people living with diabetes worldwide is projected to increase to 693 million by 2045 [1]. Diabetic nephropathy affects approximately 40% of people with diabetes and has emerged as a leading cause of chronic kidney disease (CKD) worldwide [2]; however, most patients actually die from cardiovascular disease and infections before they need renal replacement therapy [3].

Empagliflozin (Jardiance®) is a potent and highly selective inhibitor of sodium glucose cotransporter 2 (*SGLT2*), which inhibits the reabsorption of glucose in the proximal tubule of the kidney by inhibiting *SGLT2*. Empagliflozin provides a novel insulin-independent mechanism for lowering blood sugar has been developed [4]. In addition to lowering blood sugar, empagliflozin had a favorable effect on several nonglycemic outcomes, including modest reductions in body weight, blood pressure, and major adverse cardiovascular events (55% relative risk reduction in the risk empagliflozin group); Empagliflozin was approved by the European Medicines Agency (EMA) and the U.S. Food and Drug Administration (FDA) in 2014.

Research has shown that empagliflozin has multiple protective functions in cardiovascular disease research [5–7]. Empagliflozin improves diabetic myocardial structure and function, reduces myocardial oxidative stress, and improves myocardial fibrosis. Further studies have shown that empagliflozin inhibits oxidative stress and fibrosis by transforming growth factor beta→TGF-β, adenosine triphosphate→ATP, and less reactive oxygen species→ROS [8, 9].

Treatment with empagliflozin inhibits the production of inflammatory factors and reverses changes in redox parameters (e.g., glutathione and lipid peroxides), attenuates the levels of the protein kinase GIα, improves myofilament function, reduces cardiomyocyte stiffness and increases the diastolic capacity of the heart [10]. In a mouse model of ventricular fibrillation-induced cardiac arrest [11], treatment with ipagliflozin improved left ventricular function and increased survival time. GLT2 inhibitors affect lipid metabolism at several different levels, reducing lipid oxidation and shifting the utilization of substrates to the use of ketone bodies, which are more efficient for myocardial metabolism, and that less reactive oxygen species pass through these ketone bodies, affecting β-oxidation and the transport of lipid molecules in cells [12]. Despite these promising findings, there has been a lack of systematic analysis of the effects of empagliflozin on cardiac protein expression and signaling pathways.

In this study, we conducted proteomic analysis of heart tissue from the healthy group, disease group, and medication group to investigate the regulatory mechanism of empagliflozin at the cardiac proteome level.

Results

Quality control of samples

We evaluated cardiac collagen levels in a total of 17 mice as illustrated in Fig. 1A, which were categorized into three groups: 4 mice in the healthy group (db/m), 6 mice in the disease model group (db/db), and 7 mice in the EMPA-treated group (EMPA-treated) (Supplementary Excel Table 1). Protein integrity was assessed via SDS–PAGE combined with Coomassie brilliant blue staining, as demonstrated in Supplementary Fig. 1. The observed sample were clearly defined, and the distribution of protein molecular weights was uniform, as depicted in Supplementary Fig. 1. LC–MS-based quantitative proteomics was conducted on each sample individually, and the resulting data were analyzed via computer software. Supplementary Figure Figs. 2 and 3 present the chromatograms of all the samples. As shown in the figure, the chromatographic separation peaks of all the samples had relatively stable retention times, uniform peptide peak time distributions, and chromatographic peaks. Narrow, sharp and symmetrical without obvious trailing. By counting the number of peptide missed cleavage sites and the proportion of the corresponding total ion current intensity, the enzyme cleavage efficiency of the experiment was approximately evaluated. The total number of identified peptides was 32,701, the number of missed cleavage sites >=2 was 158, and the missed cleavage ratio was 0.48. %, and the enzymatic hydrolysis efficiency was 99.52%.

Differential protein analysis

Through PCA analysis, we found that the sample group was within the 95% confidence interval (Hotelling's T-squared ellipse), which met the statistical requirements (Supplementary Fig. 4). In addition, we also used PCA analysis to select the top 200 highly variable proteins, that were significantly different among the three groups (Fig. 1C). The comparison strategy is as follows: A total of 2 groups are compared, namely, the Empa (EMPA-treated) group versus the db/db (model) group and the db/db group versus the db/m (healthy) group. We used statistical methods to screen for differentially expressed proteins, and the screening criteria for differentially expressed proteins were Student's t-test P-value < 0.05 and FOLD CHANGE < 0.83 or FOLD CHANGE > 1.2. The original results of the difference analysis are shown in the Supplementary Table 1. Compared those in with the normal group, 213 proteins were downregulated and 228 proteins were highly expressed in the model group.

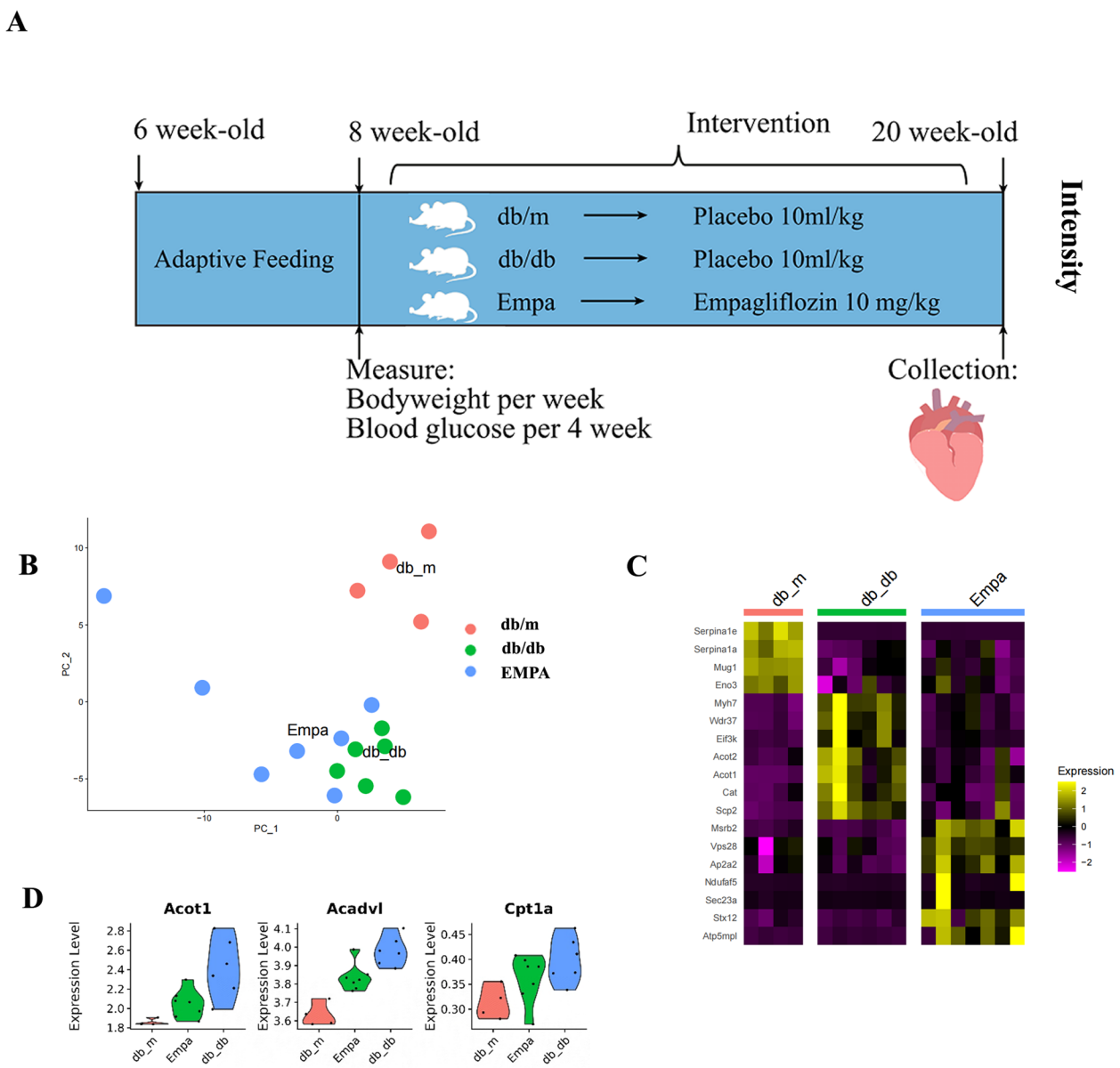

Fig. 1 Proteomic analysis of differences in cardiac tissue before and after drug treatment. (**A**) Experimental grouping design. (**B**) PCA clustering diagrams for three sample groups. (**C**) Heatmap of differentially expressed proteins. (**D**) Expression levels of ACOX1, ACADVL and CPT1A proteins in the three sample groups

The top highly expressed proteins in the model group were Myh7, Wdr37, Eif3k, Acot1, Acot2, Cat and Scp2 in the model group (Fig. 1D). With drug treatment, the increase in protein expression in the model group was reversed.

Signaling pathways of the differentially expressed proteins

To determine the changes in the signaling pathways of heart proteins in mice before and after taking empagliflozin treatment, we conducted a multidimensional signal dimension analysis, which included clusters of orthologous groups for eukaryotic complete genomes (KOG), Kyoto Encyclopedia of Genes and Genomes (KEGG), and Gene Ontology (GO) analyses. The details are as follows.

We performed KOG analysis on the differentially expressed proteins (Fig. 2). The proteins exhibiting differential expression between the disease and healthy groups were predominantly predominantly enriched in several key categories: posttranslational modification and chaperone protein turnover, lipid transport and metabolism,

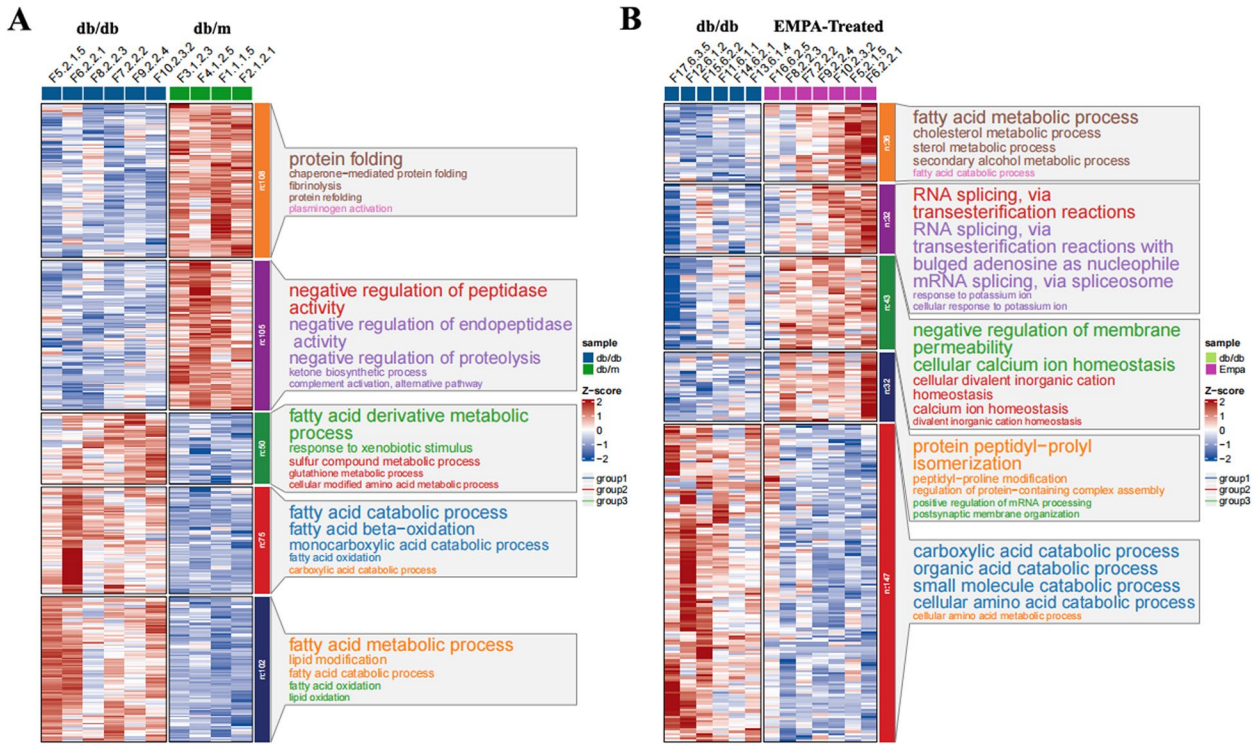

Fig. 2 KOG analysis of differentially expressed proteins between the db/m and db/db groups (**A**) and between the db/db and EMPA-treated groups (**B**)

and signal transduction mechanisms. Specifically, 47, 59, and 58 differentially expressed proteins were identified and enriched in these respective categories. (Fig. 2A). After taking the drug, the differentially expressed proteins between the disease group and the drug group were mainly enriched in mainly signal transduction mechanisms and posttranslational modification, protein turnover, and chaperones, which were enriched to 50 and 36, respectively. In the lipid transport and metabolism pathway, only 14 differentially expressed proteins were enriched (Fig. 2B). These findings indicated that the lipid transport and metabolism pathway-related proteins in cardiac tissue were significantly downregulated under the action of drugs.

Analysis of the GO (BP, biological process) pathway, revealed that the enriched upregulated ptoteins in the disease group were associated mainly withfatty acid derivative metabolism and fatty acid catabolic processes (Fig. 3A). After taking the empagliflozin treatment, the differentially expressed proteins were enriched mainly in signaling pathways such as fatty acid metabolic process, negative regulation of membrane permeability cellular calcium ion homeostasis, and RNA splicing, via transesterification reactions (Fig. 3B).

The GO analysis also revealed that the fatty acid metabolism-related proteins enriched in differential proteins in the disease group were downregulated after treatment with empagliflozin (Fig. 3). Analysis of the KEGG signaling pathways revealed that, the upregulated ptoteins in the disease group are mainly metabolic pathways and peroxisome, Protein processing in endoplasmic reticulum (Supplementary Fig. 5A). After the empagliflozin treatment, the differentially expressed proteins were mainly enriched in signaling pathways such as amyotrophic lateral sclerosis, and the enriched signaling pathways in the disease model group were altered (Supplementary Fig. 5B).

Through KOG, GO and KEGG analyses, the signaling pathways that reflect the possible effects of empagliflozin are mainly fatty acid metabolic-related signaling pathways.

Network interaction analysis of differential proteins

When proteins exercise their biological functions, they form a PPI network to maintain temporal and spatial coordination, and construct an interaction network of differentially expressed proteins, which can reveal the changing trends of differentially expressed proteins at the proteome level, and further help us identify the

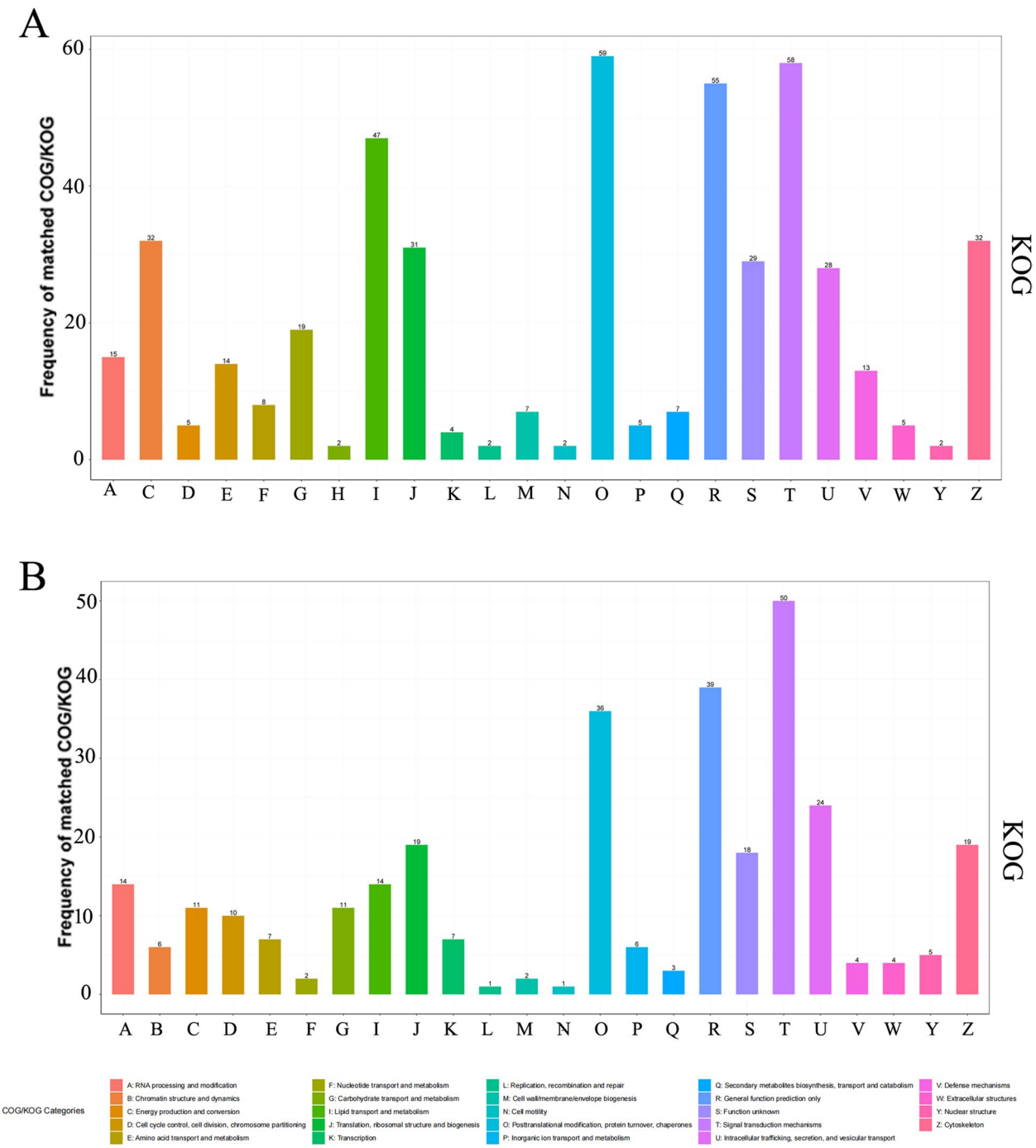

Fig. 3 GO (BP, biological process) enrichment analysis of differentially expressed proteins in each group. (**A**) db/m vs. db/db; (**B**) db/db vs. EMPA-treated

differences in differentially expressed proteins. A visual analytics platform for comprehensive gene expression profiling was used with NetworkAnalyst 3.0 (https://www.networkanalyst.ca) [13]. In the disease model group, the upregulated signaling pathways ($p < 0.05$) in heart tissue included mainly fatty acid degradation, fatty acid metabolism and peroxisome (Supplementary Excel Table 2 A) and the downregulated signaling pathways involved mainly protein processing in the endoplasmic reticulum, metabolic pathways and arginine and proline metabolism (Supplementary

A

Enriched KEGG Pathway in db/m group	Total	Expected	Hits	P.Value	FDR
Protein processing in endoplasmic reticulum	163	1.8	13	2.31E-08	7.26E-06
Arginine and proline metabolism	50	0.553	6	1.67E-05	0.00263
Metabolic pathways	1490	16.5	32	8.10E-05	0.00848

B

Enriched KEGG Pathway in db/db group	Total	Expected	Hits	P.Value	FDR
Fatty acid degradation	50	0.671	12	1.49E-12	4.69E-10
Fatty acid metabolism	57	0.765	12	8.04E-12	1.26E-09
Peroxisome	84	1.13	11	1.27E-08	0.00000113

C

Enriched KEGG Pathway in EMPA-treated group	Total	Expected	Hits	P.Value	FDR
Proteasome	46	0.455	6	5.32E-06	1.67E-03
Cell cycle	123	1.22	6	1.32E-03	0.138
TGF-beta signaling pathway	93	0.919	4	0.0133	0.598

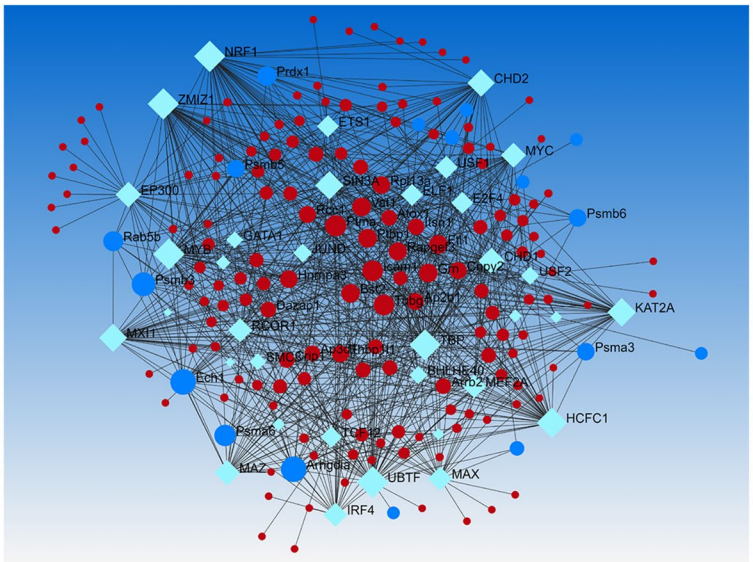

Fig. 4 Gene regulatory network analysis of differentially expressed proteins in each group. (**A**) Upregulated differential proteins between the db/m and db/db groups; (**B**) downregulated differential proteins between the db/m and db/db groups; (3) upregulated differential proteins between the db/db and EMPA-treated groups

Excel Table 2B). In addition, the significantly enriched involved were *Acox1*, *Acadvl* and *Cpt1a*. The transcription factors involved are mainly: *Chd1*, *Jund*, *Rcor1*, *Tbp*, *Gata1*, *Ubtf*, *Sin3a*, *Ep300*, *Mef2* and *Hcfc1*(Fig. 4A and B). After EMPA treatment, the enriched pathways were mainly the proteasome, cell cycle and TGF-beta signaling pathways (Supplementary Excel Table 2 C). The main transcription factors involved are: *Zmiz1*, *Mxi1*, *Nrf1*, *Chd2* and *Irf4*(Fig. 4C). In other words, the empagliflozin protects mouse heart tissue primarily by modulating signaling pathways associated with fatty acids, thereby potentially reducing oxidative stress and inflammation, and promoting overall cardiac health (Fig. 5).

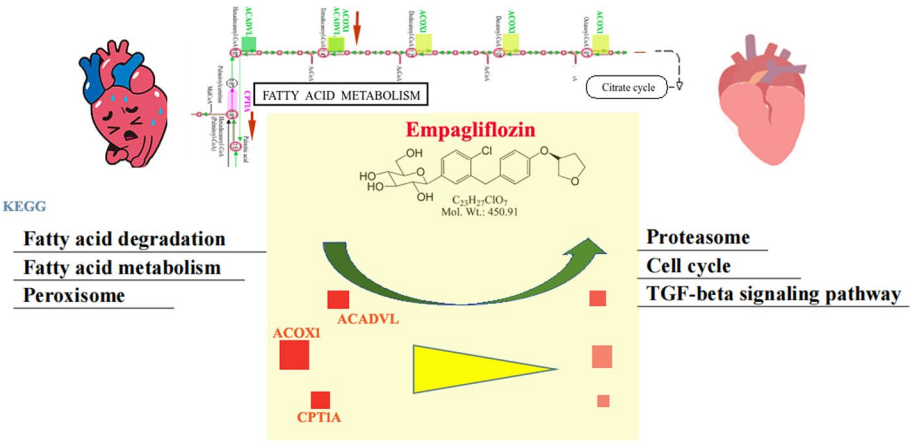

Fig. 5 Summary of the potential mechanism of action of empagliflozin

Conclusions

On the basis of our observations in mouse models, we have identified specific protein markers associated with the diabetes model group, namely Myh7, Wdr37, Eif3k, Acot1, Acot2, Cat and Scp2. Furthermore, our findings suggest that empagliflozin primarily modulates the fat-related metabolic signaling pathway in the heart. According to the results of the bioinformatics analysis, *Acox1*, *Acadvl* and *Cpt1a* may be involved in regulating the transcription factors associated with the reversal of the metabolic pathway. Collectively, our evidence from a mouse model indicates that empagliflozin affects heart tissue by targeting molecular metabolism and the fatty acid signaling pathway, thereby influencing the molecular function of the heart. However, further research is warranted to fully understand the underlying mechanisms and potential therapeutic implications.

Discussion

The underlying mechanism behind the beneficial effects of *SGLT2* inhibitors in patients at high risk of cardiovascular disease remains poorly understood. To investigate and compare the impact of hypoglycemic agents on ventricular electrophysiological substrates in metabolic mice, the relationship between adipocytokines present in pericardial fat and arrhythmia has been explored through electrophysiological techniques. These adipocytokines can contribute to an increase in the area of fibrosis area within the heart and ventricular tissues of patients diagnosed with metabolic syndrome [14, 15] and SGLT2 inhibitors can reduce the amount of pericardium fat [16–18], and can alter autonomic nervous function [19, 20]. Previous studies have also shown that SGLT2 inhibitors improve mitochondrial function in diabetic rats [21, 22]. Empagliflozin regulates the effect of adipocytokines in adipose tissue on the ion current of cardiomyocytes and reduces arrhythmia [23], which may provide a possible mechanism for antiarrhythmic effects [24]. Metabolic syndrome-induced cardiac fibrosis [25, 26] may be because adipose tissue in visceral fat resides in macrophages, producing more proinflammatory cytokines [26–28], and causing arrhythmia [29, 30]. However, the effects of SGLT2 inhibitors, especially empagliflozin, on ventricular electrophysiological substrates have not been fully elucidated.

In this study, we utilized animal models to assess the impact of drugs on the hearts of mice and identified specific cardiac protein markers associated with diabetes models in mice. Additionally, through the utilization of mass spectrometry technology, we discovered that the protective effects of empagliflozin on the hearts of mice were mediated through metabolic signaling pathways. Overall, the drugs investigated in this study were found to intervene in cardiac tissue metabolism and peroxiproteasome signaling, with a close involvement of genes related to fat metabolism. Specifically, we focused on three genes associated with fat metabolism. First, peroxisomal ACOX1 (Acyl-CoA oxidase 1) was identified as the initial and rate-limiting enzyme in fatty acid β-oxidation. ACOX1 serves as a significant source of H2O2 production, and dysfunction of ACOX1 has been associated with peroxide enzyme dioxin dyads. The protein in the CPT1 family, CPT1A-mediated lipid oxidation, also has potential as a therapeutic target [31–33]. In the context of cancer, CPT1A can mediate the fatty acid oxidation pathway [31] and can also inhibit colorectal cancer cell metastasis by inhibiting inactivation; O-GlcNAcylation regulates long-chain fatty acid metabolism by inhibiting ACOX1 ubiquitination-dependent degradation [34]. ACOX1 complexes are also new targets for liver lipid metabolism disorders induced by perfluoroalkyl and perfluoroalkyl substances [35]. High methylation of ACADVL is

associated with reduced cardiac fibrosis in patients with high-intensity interval training-related heart failure [35]. These three genes are closely correlated with fatty acid metabolism from the perspectives of cytology and tissue organs and are expected to become targets.

The expression of the CPT1A gene is tightly regulated by hormones and diet in tissues that rely heavily on fatty acid utilization, such as the heart. The regulation of CPT1A is a complex process and has been implicated in various diseases, including genetic mutations, metabolic disorders, and cancer. However, the majority of the existing data on CPT1A regulation have been derived from animal studies [32]. Furthermore, reduced expression of CPT1A has been shown to impair the cells' capacity of cells to produce aspartate, which is an essential nucleotide precursor for DNA synthesis [36].

Mutations in the ACADVL gene result in very long-chain acyl-CoA dehydrogenase deficiency, a severe and potentially life-threatening disorder affecting mitochondrial fatty acid oxidative metabolism [37]. Further research is necessary to explore the potential of targeting three specific genes in the drug signaling pathway for intervention purposes.

Methods

Sample information

In accordance with previous studies [38], male db/db mice (C57BLKS/J-leprdb/leprdb) and matched littermate db/m mice (C57BLKS/J-leprdb/leprm) were obtained from the Nanjing University Experimental Animal Center. The db/db mice were 6 weeks old and numbered 30, whereas the db/m mice served as healthy controls and numbered 15. After a 2-week adaptation period, the db/db mice were randomly divided into two groups: the db/db (disease model) group and the empagliflozin (EMPA-treated) group, with each group consisting of 15 mice. The mice in the EMPA-treated group received a daily oral gavage of 10 mg/kg EMPA daily via oral gavage for 12 weeks. Similarly, the mice in the model and control groups were administered 10 mL/kg of sterile water via the same method. After the 12-week treatment period, heart tissue samples were collected from the mice. All experimental procedures in this study were conducted in compliance with the National Law for Laboratory Animal Experimentation and were approved by the Commission on Experimental Animal Ethics of Jinan University (No. 202069-04). A total of 17 heart tissue samples from mice were included in the proteomic analysis, comprising the db/db group (6 samples), db/m group (4 samples), and EMPA-treated group (7 samples).

Sample preparation

(1) Sample preparation: An appropriate amount of sample and was placed on dry ice. The sample was transferred to a 2 mL EP tube and add 300 μL of RIPA working solutionwas added. The samples were sonicated in an ice–water bath via a cell sonicator for 2 min.The tube was centrifuged at 4 °C and 12,000 rpm for 10 min. The clear supernatant was carefully removed. (2) Protein concentration determination: Perform a BCA assay was performed to calculate the protein concentration of each sample. (3) Acetone precipitation: 100 μg of total protein was taken from each sample and diluted with H2O to a concentration of approximately 1 mg/mL. The acetone was precooled to 20 °C, and 5 times the volume of acetone was added to the sample. The mixture was mixed well, and the sample was precipitated at 20 °C overnight. The tube was centrifuged at 4 °C and 12,000 rpm for 10 min. The supernatant was carefully removed, and the pellet was rinsed twice with 200 μL of precooled 80% acetone. The mixture was centrifuged again at 12,000 rpm, and the supernatant was carefully removed. (4) Protein reconstitution, reduction, and alkylation: 100 μL of reconstituted protein mixture was added to the precipitated protein. The samples were sonicated in a water bath for 5 min to dissolve the protein precipitate. DTT was added to a final concentration of 5 mM, and the sample was incubated at 55 °C with shaking for 10 min to reduce disulfide bonds. The samples were cooled to room temperature, and IAA was added to a final concentration of 10 mM. The sample was reacted in the dark for 15 min to alkylate the reduced disulfide bonds. (5) Protein digestion: Trypsin was dissolved to a concentration of 0.5 μg/μL with resuspension buffer. The trypsin solution was incubated at room temperature for 5 min. Trypsin was mixed with each sample thoroughly at a ratio of trypsin to protein of 1:50. The mixture was incubated overnight at 37 °C with shaking at 1000 rpm after brief centrifugation. (6) SDC cleanup: TFA was added to the mixed sample to a final concentration of 2%, ensuring a pH below 2. The mixture was mixed well to precipitate SDC. The tube was centrifuged at high speed for 10 min, and the supernatant was transferred to a new EP tube. Next, 100 μL of 2% TFA was added, and the mixture was mixed thoroughly. The mixture was centrifuged at 13,000 rpm for 10 min to extract the coprecipitated polypeptides. This extraction process was repeated twice. The three supernatant fractions were combined and centrifuged at high speed for 10 min. The supernatant was transferred to a new EP tube to obtain labeled peptide samples. (7) Peptide desalting: A C18 cartridge was used following the provided instructions. The eluate was dried under vacuum at 4 °C overnight.

nanoLCMS/MS analysis

Each sample was subjected to separation and analysis via a nano-UPLC (EASYnLC1200) coupled to a Q Exactive HFX Orbitrap instrument (Thermo Fisher Scientific) with a nanoelectrospray ion source. The separation was carried out via a reversed-phase column (100 ID ×15 cm, ReprosilPur 120 C18AQ, 1.9, Dr. Math). The mobile phases consisted of H_2O with 0.1% formic acid and 2% acetonitrile (phase A) and 80% acetonitrile with 0.1% formic acid (phase B). Sample separation was performed via a 120-minute gradient at a flow rate of 300 nL/min. The gradient for phase B was as follows: 2–5% for 2 min, 5–22% for 88 min, 22–45% for 26 min, 45–95% for 2 min, and 95% for 2 min. Data-dependent acquisition (DDA) was carried out in profile and positive mode using the Orbitrap analyzer at a resolution of 120,000 (@200 m/z) and a m/z range of 350–1600 for MS1. For MS2, the resolution was set to 15,000 with a dynamic first mass. The automatic gain control (AGC) target for MS1 was set to 3E6 with a maximum injection time of 50 ms, whereas for MS2, it was set to 1E5 with a maximum injection time of 110 ms. The top 20 most intense ions were fragmented by higher-energy collisional dissociation (HCD) with a normalized collision energy (NCE) of 27% and an isolation window of 1.2 m/z. A dynamic exclusion time window of 45 s was applied, and single charged peaks and peaks with a charge exceeding 6 were excluded from the DDA procedure.

Proteome Discoverer database search

The raw MS files acquired from the vendor were processed with Proteome Discoverer (PD) software, version 2.4.0.305, employing the Sequest HT search engine. MS spectra lists were queried against species-specific UniProt FASTA databases (uniport-Mus + musculus-10090-2020-10.fasta) at the species level. The following modifications were considered during the search: carbamidomethyl [C] as a fixed modification, Oxidation (M), and acetyl (protein N-term) as variable modifications. Trypsin was selected as the protease. The peptide tolerance was set to 10 ppm, and the MS/MS tolerance was set to 0.02 Da. Up to 2 missed cleavages were allowed during the search. The false discovery rate (FDR) was set to 0.01 for both peptide-spectrum matches (PSMs) and peptide levels. For protein quantification, unique peptides and Razor peptides were used, while the total peptide amount was used for normalization. All other parameters were set to the default settings.

PCA

Using R (version 3.6.3) or SIMCA software (V16.0.2, Sartorius Stedim Data Analytics AB, Umea, Sweden), the data were logarithmically and centered, and then modeled for analysis [39].

Screening of differentially expressed proteins

We used statistical methods to screen differentially expressed proteins, where the screening criteria for differentially expressed proteins were Student's t-test *P*-VALUE < 0.05 and FOLD CHANGE < 0.83 or FOLD CHANGE > 1.2 [40].

KOG

Cluster of orthologous groups (COG) analysis is a method used to classify gene products based on their homology and functional classification. In this study, we conducted a differential protein analysis using the KOG (euKaryotic Orthologous Groups) database, which is a variant of COG analysis specifically designed for eukaryotes. This analysis was performed based on basis of the methodology described in the authors' previous literature [41]. The results of the KOG analysis for differentially expressed proteins were visualized via a histogram or bar plot [42].

GO and KEGG

For functional enrichment analysis, we utilized the Gene Ontology (GO) database, available at geneontology.org. In this project, we mapped the genes to the corresponding nodes in the Gene Ontology database and performed functional enrichment analysis using the GO database [43]. This allowed us to classify the differentially expressed proteins into their respective functional categories.

Additionally, we utilized the Kyoto Encyclopedia of Genes and Genomes (KEGG) pathway database (https://www.kegg.jp/kegg/pathway.html.) to analyze the metabolic pathways associated with the differentially expressed proteins. The KEGG database provides functional information on genes and genomes, including cellular biochemical processes such as metabolism, membrane transport, signaling, cell cycle, and conserved sub-pathways. By identifying the metabolic pathways that are significantly enriched with differentially expressed proteins, we can gain insights into the systematic alterations occurring under different experimental conditions.

Analysis of gene regulatory networks build

For gene regulatory network analysis, we employed NetworkAnalyst (https://www.networkanalyst.ca), a web-based tool that allows researchers to perform various meta-analyses on gene expression data [13]. In our project, we used the differentially expressed proteins for the analysis and selected specific parameters. The organism

was specified as *Mus musculus*, and the gene regulatory network (GRN) database utilized was the TF–gene interaction database from ENCODE. The ENCODE database provides transcription factor and gene target data derived from ChIP-seq data. Only peak intensity signals less than 500 and predicted regulatory potential scores less than 1 were used, employing the BETA Minus algorithm.

Supplementary Information

The online version contains supplementary material available at https://doi.org/10.1186/s12953-024-00232-1.

Additional file 1: Supplementary Excel Table 1: Analysis of protein expression levels and differences in each sample; Supplementary Excel Table 2 :KEGG enrichment results obtained from network interaction analysis of differential proteins; Supplementary table1 :Sample information.

Additional file 2: Supplementary table2: KOG catalog.

Additional file 3: Supplementary figure 1: SDS-PAGE and Coomassie brilliant blue staining of 17 samples; Supplementary figure 2: Total ion chromatograms for each sample grouping; Supplementary figure 3: Total Ion Chromatography and Base Peak Chromatogram of 17 samples; Supplementary figure 4: Score scatter plot for PCA model; Supplementary figure 5: KEGG enrichment analysis of differential proteins in each group.

Authors' contributions

All the authors discussed the results and contributed to the fifinal manuscript. All authors have read and agreed to the published version of the manuscript.

Funding

This work was supported by the Project of Administration of Traditional Chinese Medicine of Guangdong Province of China (No. 20232025).

Availability of data and materials

The original chromatograms of the proteome are attached, and the original proteome file can be obtained from the author. The author's email address is zhangh355@mail2.sysu.edu.cn.

Data availability

No datasets were generated or analysed during the current study.

Declarations

Ethics approval and consent to participate

All experimental procedures in this study were conducted in compliance with the National Law for Laboratory Animal Experimentation and were approved by the Commission on Experimental Animal Ethics of Jinan University (No. 202069-04).

Competing interests

The authors declare no competing interests.

Received: 3 January 2024 Accepted: 23 September 2024
Published online: 19 October 2024

References

1. Khan MZ, Hussain M, Khan AA, Hassan U, Akhter N, Hameed M, Mushtaq S, Awan UA. Frequency of non-diabetic renal disease in type 2 diabetes mellitus patients undergoing renal biopsy. J Ayub Med Coll Abbottabad. 2021;33(Suppl 1):S757–62.
2. Obrador GT, Levin A. CKD hotspots: challenges and areas of opportunity. Semin Nephrol. 2019;39(3):308–14. https://doi.org/10.1016/j.semnephrol.2019.02.009.
3. Alicic RZ, Rooney MT, Tuttle KR. Diabetic kidney disease: challenges, progress, and possibilities. Clin J Am Soc Nephrol. 2017;12(12):2032–45. https://doi.org/10.2215/CJN.11491116.
4. Frampton JE, Empagliflozin. A review in type 2 diabetes. Drugs 78 (10), 1037–48. https://doi.org/10.1007/s40265-018-0937-z.
5. Cooper S, Teoh H, Campeau MA, Verma S, Leask RL. Empagliflozin restores the integrity of the endothelial glycocalyx in vitro. Mol Cell Biochem. 2019;459(1–2):121–30. https://doi.org/10.1007/s11010-019-03555-2.
6. Lytvyn Y, Bjornstad P, Udell JA, Lovshin JA, Cherney D. Sodium glucose cotransporter-2 inhibition in heart failure: potential mechanisms, clinical applications, and summary of clinical trials. Circulation. 2017;136(17):1643–58. https://doi.org/10.1161/CIRCULATIONAHA.117.030012.
7. Shao Q, Meng L, Lee S, Tse G, Gong M, Zhang Z, Zhao J, Zhao Y, Li G, Liu T. Empagliflozin, a sodium glucose co-transporter-2 inhibitor, alleviates atrial remodeling and improves mitochondrial function in high-fat diet/streptozotocin-induced diabetic rats. Cardiovasc Diabetol. 2019a;18(1):165. https://doi.org/10.1186/s12933-019-0964-4.
8. Li C, Zhang J, Xue M, Li X, Han F, Liu X, Xu L, Lu Y, Cheng Y, Li T, Yu X, Sun B, Chen L. SGLT2 inhibition with empagliflozin attenuates myocardial oxidative stress and fibrosis in diabetic mice heart. Cardiovasc Diabetol. 2019;18(1):15. https://doi.org/10.1186/s12933-019-0816-2.
9. Zou R, Shi W, Qiu J, Zhou N, Du N, Zhou H, Chen X, Ma L. Empagliflozin attenuates cardiac microvascular ischemia/reperfusion injury through improving mitochondrial homeostasis. Cardiovasc Diabetol. 2022;21(1):106. https://doi.org/10.1186/s12933-022-01532-6.
10. Kolijn D, Pabel S, Tian Y, Lodi M, Herwig M, Carrizzo A, Zhazykbayeva S, Kovacs A, Fulop GA, Falcao-Pires I, Reusch PH, Linthout SV, Papp Z, van Heerebeek L, Vecchione C, Maier LS, Ciccarelli M, Tschope C, Mugge A, Bagi Z, Sossalla S, Hamdani N. Empagliflozin improves endothelial and cardiomyocyte function in human heart failure with preserved ejection fraction via reduced pro-inflammatory-oxidative pathways and protein kinase galpha oxidation. Cardiovasc Res. 2021;117(2):495–507. https://doi.org/10.1093/cvr/cvaa123.
11. Tan Y, Yu K, Liang L, Liu Y, Song F, Ge Q, Fang X, Yu T, Huang Z, Jiang L, Wang P. Sodium-glucose co-transporter 2 inhibition with empagliflozin improves cardiac function after cardiac arrest in rats by enhancing mitochondrial energy metabolism. Front Pharmacol. 2021;12:758080. https://doi.org/10.3389/fphar.2021.758080.
12. Qiu H, Novikov A, Vallon V. Ketosis and diabetic ketoacidosis in response to SGLT2 inhibitors: Basic mechanisms and therapeutic perspectives. Diabetes Metab Res Rev. 2017;33(5). https://doi.org/10.1002/dmrr.2886.
13. Zhou G, Soufan O, Ewald J, Hancock R, Basu N, Xia J. NetworkAnalyst 3.0: a visual analytics platform for comprehensive gene expression profiling and meta-analysis. Nucleic Acids Res. 2019;47(W1):W234–41. https://doi.org/10.1093/nar/gkz240.
14. Wong CX, Ganesan AN, Selvanayagam JB. Epicardial fat and atrial fibrillation: current evidence, potential mechanisms, clinical implications, and future directions. Eur Heart J. 2017;38(17):1294–302. https://doi.org/10.1093/eurheartj/ehw045.
15. Sanchez J, Gomez JF, Martinez-Mateu L, Romero L, Saiz J, Trenor B. Heterogeneous effects of fibroblast-myocyte coupling in different regions of the human atria under conditions of atrial fibrillation. Front Physiol. 2019;10:847. https://doi.org/10.3389/fphys.2019.00847.
16. Tam WC, Lin YK, Chan WP, Huang JH, Hsieh MH, Chen SA, Chen YJ. Pericardial fat is associated with the risk of ventricular arrhythmia in Asian patients. Circ J. 2016;80(8):1726–33. https://doi.org/10.1253/circj.CJ-16-0047.
17. Chang D, Zhang S, Yang D, Gao L, Lin Y, Chu Z, Jiang X, Yin X, Zheng Z, Wei X, You D, Xiao X, Cong P, Bian X, Xia Y, Yang Y. Effect of epicardial fat pad ablation on acute atrial electrical remodeling and inducibility of atrial fibrillation. Circ J. 2010;74(5):885–94. https://doi.org/10.1253/circj.cj-09-0967.
18. Saxon DR, Rasouli N, Eckel RH. Pharmacological prevention of cardiovascular outcomes in diabetes mellitus: established and emerging agents. Drugs. 2018;78. https://doi.org/10.1007/s40265-017-0857-3.

19. Jhuo SJ, Liu IH, Tasi WC, Chou TW, Lin YH, Wu BN, Lee KT, Lai WT. Characteristics of ventricular electrophysiological substrates in metabolic mice treated with empagliflozin. Int J Mol Sci. 2021;22(11). https://doi.org/10.3390/ijms22116105.
20. Inzucchi SE, Zinman B, Wanner C, Ferrari R, Fitchett D, Hantel S, Espadero RM, Woerle HJ, Broedl UC, Johansen OE. SGLT-2 inhibitors and cardiovascular risk: proposed pathways and review of ongoing outcome trials. Diab Vasc Dis Res. 2015;12(2):90–100. https://doi.org/10.1177/1479164114559852.
21. Shao Q, Meng L, Lee S, Tse G, Gong M, Zhang Z, Zhao J, Zhao Y, Li G, Liu T. Empagliflozin, a sodium glucose co-transporter-2 inhibitor, alleviates atrial remodeling and improves mitochondrial function in high-fat diet/streptozotocin-induced diabetic rats. Cardiovasc Diabetol. 2019b;18(1):165. https://doi.org/10.1186/s12933-019-0964-4.
22. Ring A, Brand T, Macha S, Breithaupt-Groegler K, Simons G, Walter B, Woerle HJ, Broedl UC. The sodium glucose cotransporter 2 inhibitor empagliflozin does not prolong QT interval in a thorough QT (TQT) study. Cardiovasc Diabetol. 2013;12:70. https://doi.org/10.1186/1475-2840-12-70.
23. Lee KT, Tang PW, Tsai WC, Liu IH, Yen HW, Voon WC, Wu BN, Sheu SH, Lai WT. Differential effects of central and peripheral fat tissues on the delayed rectifier K(+) outward currents in cardiac myocytes. Cardiology. 2013;125(2):118–24. https://doi.org/10.1159/000350360.
24. Jhuo SJ, Liu IH, Tsai WC, Chou TW, Lin YH, Wu BN, Lee KT, Lai WT. Effects of Secretome from Fat Tissues on Ion currents of Cardiomyocyte modulated by sodium-glucose transporter 2 inhibitor. Molecules. 2020;25(16). https://doi.org/10.3390/molecules25163606.
25. Lee HC, Chen CC, Tsai WC, Lin HT, Shiao YL, Sheu SH, Wu BN, Chen CH, Lai WT. Very-low-density lipoprotein of metabolic syndrome modulates gap junctions and slows cardiac conduction. Sci Rep. 2017;7(1):12050. https://doi.org/10.1038/s41598-017-11416-5.
26. Ladeiras-Lopes R, Moreira HT, Bettencourt N, Fontes-Carvalho R, Sampaio F, Ambale-Venkatesh B, Wu C, Liu K, Bertoni AG, Ouyang P, Bluemke DA, Lima JA. Metabolic syndrome is associated with impaired diastolic function independently of MRI-Derived myocardial extracellular volume: the MESA study. Diabetes. 2018;67(5):1007–12. https://doi.org/10.2337/db17-1496.
27. Hamdy O, Porramatikul S, Al-Ozairi E. Metabolic obesity: the paradox between visceral and subcutaneous fat. Curr Diabetes Rev. 2006;2(4):367–73. https://doi.org/10.2174/1573399810602040367.
28. Pellman J, Zhang J, Sheikh F. Myocyte-fibroblast communication in cardiac fibrosis and arrhythmias: mechanisms and model systems. J Mol Cell Cardiol. 2016;94:22–31. https://doi.org/10.1016/j.yjmcc.2016.03.005.
29. Adamsson ES, Smith JG, Melander O, Hedblad B, Engstrom G. Inflammation-sensitive proteins and risk of atrial fibrillation: a population-based cohort study. Eur J Epidemiol. 2011;26(6):449–55. https://doi.org/10.1007/s10654-011-9565-6.
30. Hu YF, Yeh HI, Tsao HM, Tai CT, Lin YJ, Chang SL, Lo LW, Tuan TC, Tzeng CH, Huang SH, Lin YK, Chen SA. Impact of circulating monocyte CD36 level on atrial fibrillation and subsequent catheter ablation. Heart Rhythm. 2011;8(5):650–6. https://doi.org/10.1016/j.hrthm.2010.12.036.
31. Liu Z, Liu W, Wang W, Ma Y, Wang Y, Drum DL, Cai J, Blevins H, Lee E, Shah S, Fisher PB, Wang X, Fang X, Guo C, Wang XY. CPT1A-mediated fatty acid oxidation confers cancer cell resistance to immune-mediated cytolytic killing. Proc Natl Acad Sci U S A. 2023;120(39):e1992089176. https://doi.org/10.1073/pnas.2302878120.
32. Schlaepfer IR, Joshi M. CPT1A-mediated fat oxidation, mechanisms, and therapeutic potential. Endocrinology. 2020;161(2). https://doi.org/10.1210/endocr/bqz046.
33. Wang YN, Zeng ZL, Lu J, Wang Y, Liu ZX, He MM, Zhao Q, Wang ZX, Li T, Lu YX, Wu QN, Yu K, Wang F, Pu HY, Li B, Jia WH, Shi M, Xie D, Kang TB, Huang P, Ju HQ, Xu RH. CPT1A-mediated fatty acid oxidation promotes colorectal cancer cell metastasis by inhibiting anoikis. Oncogene. 2018;37(46):6025–40. https://doi.org/10.1038/s41388-018-0384-z.
34. Zhang M, Zhou W, Cao Y, Kou L, Liu C, Li X, Zhang B, Guo W, Xu B, Li S. O-GlcNAcylation regulates long-chain fatty acid metabolism by inhibiting ACOX1 ubiquitination-dependent degradation. Int J Biol Macromol. 2024;266(Pt 2):131151. https://doi.org/10.1016/j.ijbiomac.2024.131151.
35. Yang W, Ling X, He S, Cui H, Yang Z, An H, Wang L, Zou P, Chen Q, Liu J, Ao L, Cao J. PPARα/ACOX1 as a novel target for hepatic lipid metabolism disorders induced by per- and polyfluoroalkyl substances: an integrated approach. Environ Int. 2023;178:108138. https://doi.org/10.1016/j.envint.2023.108138.
36. Schoors S, Bruning U, Missiaen R, Queiroz KC, Borgers G, Elia I, Zecchin A, Cantelmo AR, Christen S, Goveia J, Heggermont W, Godde L, Vinckier S, Van Veldhoven PP, Eelen G, Schoonjans L, Gerhardt H, Dewerchin M, Baes M, De Bock K, Ghesquiere B, Lunt SY, Fendt SM, Carmeliet P. Fatty acid carbon is essential for dNTP synthesis in endothelial cells. Nature. 2015;520(7546):192–7. https://doi.org/10.1038/nature14362.
37. Arunath V, Liyanarachchi MS, Gajealan S, Jasinge E, Weerasekara K, Moheb LA. A novel mutation in ACADVL causing very long-chain acyl-coenzyme-A dehydrogenase deficiency in a south Asian pediatric patient: a case report and review of the literature. J Med Case Rep. 2021;15(1):441. https://doi.org/10.1186/s13256-021-03013-y.
38. Lu YP, Zhang ZY, Wu HW, Fang LJ, Hu B, Tang C, Zhang YQ, Yin L, Tang DE, Zheng ZH, Zhu T, Dai Y. SGLT2 inhibitors improve kidney function and morphology by regulating renal metabolic reprogramming in mice with diabetic kidney disease. J Transl Med. 2022;20(1):420. https://doi.org/10.1186/s12967-022-03629-8.
39. Wiklund S, Johansson E, Sjostrom L, Mellerowicz EJ, Edlund U, Shockcor JP, Gottfries J, Moritz T, Trygg J. Visualization of GC/TOF-MS-based metabolomics data for identification of biochemically interesting compounds using OPLS class models. Anal Chem. 2008;80(1):115–22. https://doi.org/10.1021/ac0713510.
40. Liu X, Wang J, Gao L, Liu H, Liu C. ITRAQ-Based proteomic analysis of neonatal kidney from offspring of protein restricted rats reveals abnormalities in intraflagellar transport proteins. Cell Physiol Biochem. 2017;44(1):185–99. https://doi.org/10.1159/000484626.
41. Zhang H, Fu Y, Wang L, Liang A, Chen S, Xu A. Identifying novel conopeptides from the venom ducts of Conus Litteratus through integrating transcriptomics and proteomics. J Proteom. 2019;192:346–57. https://doi.org/10.1016/j.jprot.2018.09.015.
42. Huerta-Cepas J, Szklarczyk D, Heller D, Hernandez-Plaza A, Forslund SK, Cook H, Mende DR, Letunic I, Rattei T, Jensen LJ, von Mering C, Bork P. EggNOG 5.0: a hierarchical, functionally and phylogenetically annotated orthology resource based on 5090 organisms and 2502 viruses. Nucleic Acids Res. 2019;47(D1):D309–14. https://doi.org/10.1093/nar/gky1085.
43. Huang DW, Sherman BT, Lempicki RA. Systematic and integrative analysis of large gene lists using DAVID bioinformatics resources. Nat Protoc. 2009;4(1):44–57. https://doi.org/10.1038/nprot.2008.211.

Publisher's note